J|A|C|S ARTICLES

Published on Web 07/17/2009

Monomeric Copper(I), Silver(I), and Gold(I) Alkyne Complexes and the Coinage Metal Family Group Trends

H. V. Rasika Dias,* Jaime A. Flores, Jiang Wu, and Peter Kroll*

Department of Chemistry and Biochemistry, The University of Texas at Arlington, Arlington, Texas 76019

Received May 26, 2009; E-mail: dias@uta.edu

Abstract: A series of thermally stable, easily isolable, monomeric, and isoleptic coinage metal alkyne complexes have been reported. Treatment of $[N\{(C_3F_7)C(Dipp)N\}_2]Li$ (the lithium salt of the 1,3,5-triazapentadiene $[N\{(C_3F_7)C(Dipp)N\}_2]H$) with AuCl, CF_3SO_3Ag or CF_3SO_3Cu in the presence of 3-hexyne led to the corresponding coinage metal alkyne complex $[N\{(C_3F_7)C(Dipp)N\}_2]M(EtC{\equiv}CEt)$ in good yield (M = Au, Ag, Cu; Dipp = 2,6-diisopropylphenyl). X-ray crystal structures of the three coinage metal alkynes are remarkably similar, and show the presence of trigonal-planar metal sites with η^2-bonded 3-hexyne. The M−C and M−N bond distances vary in the order Cu < Au < Ag. The bending of the C−C≡C bond angle is largest for the gold, followed by Cu and Ag adducts. The gold adduct also shows the largest decrease in C≡C stretching frequency in Raman, while the Ag adduct shows the smallest change compared to that of the uncoordinated alkyne. DFT calculations on $[N\{(CF_3)C(Ph)N\}_2]M(EtC{\equiv}CEt)$ and the related ClM(EtC≡CEt) predict that the M−alkyne bond energy varies in the order Ag < Cu < Au. The gold adducts are also predicted to have the longest C≡C, largest deviation of C−C≡C bond angle from linearity, and smallest C≡C stretching frequency, followed by the Cu and Ag adducts. In these triazapentadienyl coinage metal adducts, the σ-donation from alkyne → M dominates over the M → alkyne π-back-donation.

Introduction

Coinage metals (Cu, Ag, Au) mediate many important transformations involving alkynes such as heteroatom−hydrogen bond additions, cycloaddition chemistry, C_{sp}−H bond functionalizations and alkyne coupling processes, and hydrogenations.[1−7] Coinage metal alkyne complexes are believed to be key intermediates in most of these reactions. Copper alkynes are also used as precursors for the copper deposition.[8,9] Gold is an excellent catalyst for the hydrochlorination of acetylene to give vinyl chloride,[10] which is an important industrial chemical. Consequently, there is a considerable interest in the isolable molecules with coinage metal alkyne bonds. They serve as good models for the likely reaction intermediates, provide useful spectroscopic and structural data, are convenient precursors for various applications, and offer valuable insights to the metal−alkyne bonding and reaction mechanisms.

A search of the Cambridge Structural Database and the current literature revealed that there is quite a number of well-characterized copper and silver alkynes.[11,12] Mononuclear systems, however, are relatively less common. Nevertheless, even a few acetylene adducts of Cu(I) and Ag(I) have been isolated and structurally characterized,[13,14] despite the known tendency of coinage metal ions to form explosive materials such as coinage metal carbides with acetylene.[15,16] In contrast, structural data on gold−alkyne complexes are extremely limited (see Figure 1) and gold−acetylene adducts are not available.[7,17] Furthermore, except for a recent report on Au(EtC≡CEt)Cl (**1**),[18] which has a simple alkyne bonded to AuCl, all the structurally authenticated gold−alkynes in the literature have strained alkynes like 3,3,6,6-tetramethyl-1-thiacycloept-4-yne-1,1-dioxide (**2**)[19] and 3,3,6,6-tetramethyl-1-thiacyclohept-4-yne (**3**)[19] or an alkyne in a tethered framework (**4**),[20] and are multinuclear species. The scarcity of detailed structural data on gold−alkynes is particularly striking since gold is fast becoming the metal of choice for effectively catalyzing many important

(1) Hashmi, A. S. K. *Chem. Rev.* **2007**, *107*, 3180–3211.
(2) Alonso, F.; Beletskaya, I. P.; Yus, M. *Chem. Rev.* **2004**, *104*, 3079–3159.
(3) Arcadi, A. *Chem. Rev.* **2008**, *108*, 3266–3325.
(4) Fuerstner, A.; Davies, P. W. *Angew. Chem., Int. Ed.* **2007**, *46*, 3410–3449.
(5) Weibel, J.-M.; Blanc, A.; Pale, P. *Chem. Rev.* **2008**, *108*, 3149–3173.
(6) Meldal, M.; Tornoe, C. W. *Chem. Rev.* **2008**, *108*, 2952–3015.
(7) Schmidbaur, H.; Schier, A. Gold Organometallics. In *Comprehensive Organometallic Chemistry III*; Elsevier: Amsterdam, 2007; Vol. 2, pp 251−307.
(8) Perez, P. J.; Dias-Requejo, M. M. Copper Organometallics. In *Comprehensive Organometallic Chemistry III*; Elsevier: Amsterdam, 2007; Vol. 2, pp 153−195.
(9) Koehler, K.; Eichhorn, J.; Meyer, F.; Vidovic, D. *Organometallics* **2003**, *22*, 4426–4432.
(10) Conte, M.; Carley, A. F.; Heirene, C.; Willock, D. J.; Johnston, P.; Herzing, A. A.; Kiely, C. J.; Hutchings, G. J. *J. Catal.* **2007**, *250*, 231–239.
(11) (a) Cambridge Crystallographic Data Center (CCDC): CSD version 5.30 (November 2008). (b) Allen, F. H. *Acta Crystallogr., Sect. B* **2002**, *B58*, 380–388.
(12) Lang, H.; Koehler, K.; Blau, S. *Coord. Chem. Rev.* **1995**, *143*, 113–168.
(13) For the first X-ray structural data on a Cu−acetylene complex, see: Thompson, J. S.; Whitney, J. F. *J. Am. Chem. Soc.* **1983**, *105*, 5488–5490.
(14) For the first X-ray structural data on a Ag−acetylene complex, see: Dias, H. V. R.; Wang, Z.; Jin, W. *Inorg. Chem.* **1997**, *36*, 6205–6215.
(15) Frad, W. A. *Adv. Inorg. Chem. Radiochem.* **1968**, *11*, 153–247.
(16) Mathews, J. A.; Watters, L. L. *J. Am. Chem. Soc.* **1900**, *22*, 108–111.

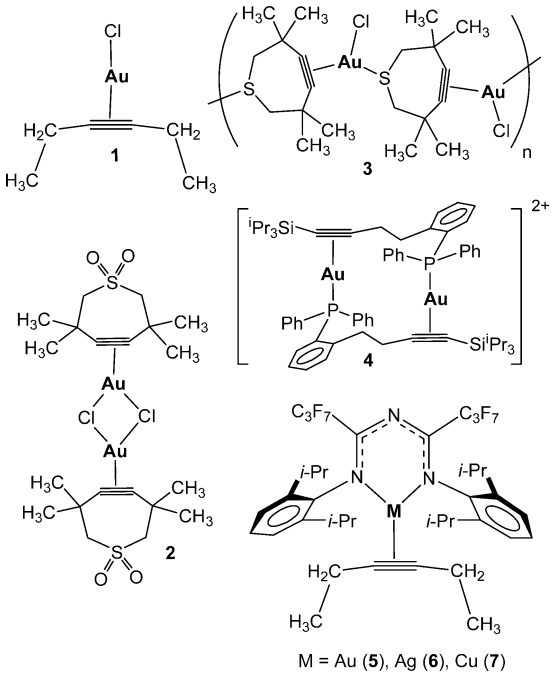

Figure 1. Structurally characterized gold(I)−alkyne complexes **1**−**4** and coinage metal alkyne adducts [N{(C$_3$F$_7$)C(Dipp)N}$_2$]M(EtC≡CEt) (M = Au, **5**; Ag, **6**; Cu, **7**) supported by a triazapentadienyl ligand.

chemical processes involving alkynes.[1−4,18,21] Here we describe the synthesis, spectroscopic and structural data of a thermally stable gold(I)−alkyne complex. In addition, we also report the analogous silver and copper adducts, thus completing the *first series of well-authenticated, isoleptic*[22,23] *coinage metal alkynes* (i.e., metal adducts with the same ligand set; see refs 22 and 23 for a more detailed description of term *isoleptic*) that are ideal for a group trend study. It is also noteworthy that these coinage metal adducts are monometallic systems and were prepared using a simple, commercially available alkyne. Fluorinated 1,3,5-triazapentadienyl anion, [N{(C$_3$F$_7$)C(Dipp)N}$_2$]$^-$ (Dipp = 2,6-diisopropylphenyl), serves as the supporting ligand in these molecules (Figures 1, **5**−**7**). Such ligands have been utilized previously to stabilize rare organometallic species involving coinage metal ions (e.g., gold(I)−ethylene adducts).[24−26]

Results and Discussion

The treatment of AuCl with [N{(C$_3$F$_7$)C(Dipp)N}$_2$]Li (prepared directly from [N{(C$_3$F$_7$)C(Dipp)N}$_2$]H and ^{n}BuLi) and 3-hexyne (EtC≡CEt) in hexane led to [N{(C$_3$F$_7$)C(Dipp)N}$_2$]Au(EtC≡CEt) (**5**) as a yellow solid. Unlike ClAu(EtC≡CEt), which rapidly decomposes upon exposure to air,[18] crystals of **5** are remarkably stable and can be left exposed to air and ambient light well over a day without any apparent decomposition. The analogous silver(I) and copper(I) adducts can also be synthesized via a similar route using CF_3SO_3Ag and CF_3SO_3Cu precursors. Solid samples of [N{(C$_3$F$_7$)C(Dipp)N}$_2$]Ag(EtC≡CEt) (**6**) and [N{(C$_3$F$_7$)C(Dipp)N}$_2$]Cu(EtC≡CEt) (**7**) can also be handled in air for some periods without any decomposition. The silver adduct **6** is relatively less stable compared to the gold analogue in solution, particularly in chlorinated solvents such as $CDCl_3$. For example, it decomposes slowly in $CDCl_3$ over a period of several hours (∼6 h) forming black deposits. In contrast, the gold adduct **5** is stable for more than 24 h under similar conditions.

^{1}H NMR spectra of **5**−**7** in $CDCl_3$ at the room temperature exhibit signals corresponding to the ethyl moieties of the alkyne at the δ 1.1−0.75 region, which is an upfield shift compared to the corresponding signals of the free 3-hexyne (δ 2.13 and 1.09). In contrast, the AuCl(EtC≡CEt) adduct showed a downfield shift of both signals. It is likely that the proton signals of the ethyl moieties in **5**−**7** are affected by the ring currents of the flanking *N*-aryl groups. The ^{13}C NMR signal of the acetylenic carbons of **5** in C_6D_{12} appears at δ 91.3 which is a downfield shift relative to that of the free ligand (δ 80.7). The AuCl(EtC≡CEt) (δ 86.4) also shows a similar downfield shifted resonance. The corresponding signals of the silver and copper adducts, **6** and **7**, in C_6D_{12} were observed at δ 80.6 and 99.2, respectively.

Compounds [N{(C$_3$F$_7$)C(Dipp)N}$_2$]M(EtC≡CEt) (M = Au (**5**), Ag (**6**), Cu (**7**)) afford X-ray quality, isomorphous crystals (note the strikingly similar unit cell dimensions) from hexane at −20 °C. X-ray structures of the three adducts are illustrated in Figures 2, 3, and 4, and key structural parameters are summarized in Table 1. Additional details are provided in the Supporting Information. The coinage metal alkyne adducts [N{(C$_3$F$_7$)C(Dipp)N}$_2$]M(EtC≡CEt) (M = Au, Ag, Cu) are monomeric molecules with very similar structures. The triazapentadienyl ligand in **5**−**7** coordinates to the coinage metal in a κ^2-fashion, forming an essentially planar six-membered, MN_3C_2 metallacycle. They all feature three-coordinate metal sites, which is particularly less common for gold.[27] The 3-hexyne coordinates to the coinage metal center in an η^2-fashion. The M−N and M−C distances increase in the order Cu < Au < Ag, which is consistent with the covalent radii of the respective monovalent ions (e.g., 1.13, 1.25, and 1.33 Å for two-coordinate copper(I), gold(I), and silver(I), respectively).[28,29] The C≡C bond lengths of the bonded alkynes in the three adducts appear to be marginally longer than the typical

(17) A limited number of gold(I)-coordinated metal alkynyls and spectroscopically detected gold−alkynes are also known: (a) Hüttel, R.; Forkl, H. *Chem. Ber.* **1972**, *105*, 1664–1673. (b) Mingos, D. M. P.; Yau, J.; Menzer, S.; Williams, D. J. *Angew. Chem., Int. Ed. Engl.* **1995**, *34*, 1894–1895. (c) Lang, H.; Koehler, K.; Zsolnai, L. *Chem. Commun.* **1996**, 2043–2044. Koehler, K.; Silverio, S. J.; Hyla-Kryspin, I.; Gleiter, R.; Zsolnai, L.; Driess, A.; Huttner, G.; Lang, H. *Organometallics* **1997**, *16*, 4970–4979. (d) Yip, S.-K.; Cheng, E. C.-C.; Yuan, L.-H.; Zhu, N.; Yam, V. W.-W. *Angew. Chem., Int. Ed.* **2004**, *43*, 4954–4957. (e) Fornies, J.; Fuertes, S.; Martin, A.; Sicilia, V.; Lalinde, E.; Moreno, M. T. *Chem.−Eur. J.* **2006**, *12*, 8253–8266. (f) Akana, J. A.; Bhattacharyya, K. X.; Mueller, P.; Sadighi, J. P. *J. Am. Chem. Soc.* **2007**, *129*, 7736–7737. (g) Zhang, S.; Chandra, K. L.; Gorman, C. B. *J. Am. Chem. Soc.* **2007**, *129*, 4876–4877. (h) Lavallo, V.; Frey, G. D.; Donnadieu, B.; Soleilhavoup, M.; Bertrand, G. *Angew. Chem., Int. Ed.* **2008**, *47*, 5224–5228.
(18) Wu, J.; Kroll, P.; Dias, H. V. R. *Inorg. Chem.* **2009**, *48*, 423–425, and references therein.
(19) Schulte, P.; Behrens, U. *Chem. Commun.* **1998**, 1633–1634.
(20) Shapiro, N. D.; Toste, F. D. *Proc. Natl. Acad. Sci. U.S.A.* **2008**, *105*, 2779–2782.
(21) Hutchings, G. J.; Brust, M.; Schmidbaur, H. *Chem. Soc. Rev.* **2008**, *37*, 1759–1765.
(22) Davidson, P. J.; Lappert, M. F.; Pearce, R. *Acc. Chem. Res.* **1974**, *7*, 209–217.
(23) Davidson, P. J.; Lappert, M. F.; Pearce, R. *Chem. Rev.* **1976**, *76*, 219–242.
(24) Dias, H. V. R.; Singh, S. *Inorg. Chem.* **2004**, *43*, 7396–7402.
(25) Dias, H. V. R.; Singh, S. *Inorg. Chem.* **2004**, *43*, 5786–5788.
(26) Flores, J. A.; Dias, H. V. R. *Inorg. Chem.* **2008**, *47*, 4448–4450.
(27) Carvajal, M. A.; Novoa, J. J.; Alvarez, S. *J. Am. Chem. Soc.* **2004**, *126*, 1465–1477.
(28) Bayler, A.; Schier, A.; Bowmaker, G. A.; Schmidbaur, H. *J. Am. Chem. Soc.* **1996**, *118*, 7006–7007.

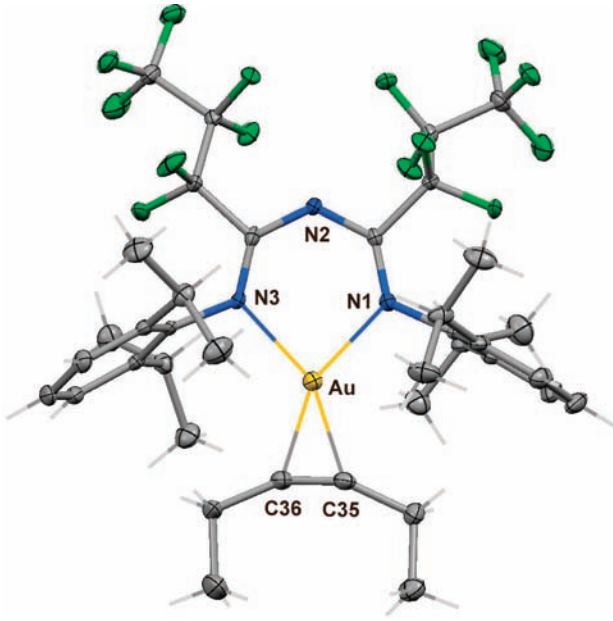

Figure 2. Molecular structure of [N{(C$_3$F$_7$)C(Dipp)N}$_2$]Au(EtC≡CEt) (**5**). Thermal ellipsoids drawn at the 50% level. Selected bond lengths (Å) and angles (deg): Au−C(35) 2.069(4), Au−C(36) 2.071(4), Au−N(1) 2.153(3), Au−N(3) 2.155(3), C(35)−C(36) 1.233(7); C(35)−Au−C(36) 34.66(18), N(1)−Au−N(3) 85.31(13), C(36)−C(35)−C(34) 155.0(4), C(35)−C(36)−C(37) 155.7(5).

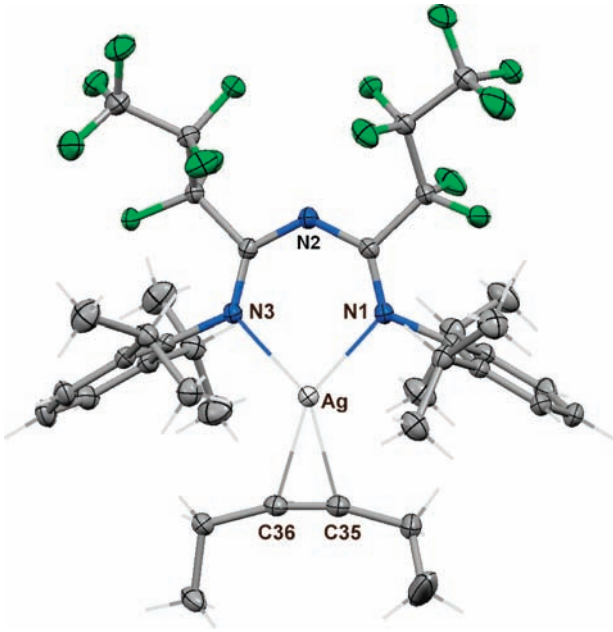

Figure 3. Molecular structure of [N{(C$_3$F$_7$)C(Dipp)N}$_2$]Ag(EtC≡CEt) (**6**). Thermal ellipsoids drawn at the 50% level. Selected bond lengths (Å) and angles (deg): Ag−N(1) 2.2026(18), Ag−N(3) 2.2027(17), Ag−C(35) 2.233(2), Ag−C(36) 2.241(2), C(35)−C(36) 1.216(3); N(1)−Ag−N(3) 85.03(6), C(35)−Ag−C(36) 31.54(8), C(36)−C(35)−C(34) 164.7(2), C(35)−C(36)−C(37) 165.3(2).

alkyne C≡C bond distance of 1.202(5) Å[30] (e.g., ^{t}BuC≡C^{t}Bu, 1.2022(15) Å),[31] with Cu and Au adducts featuring the longer

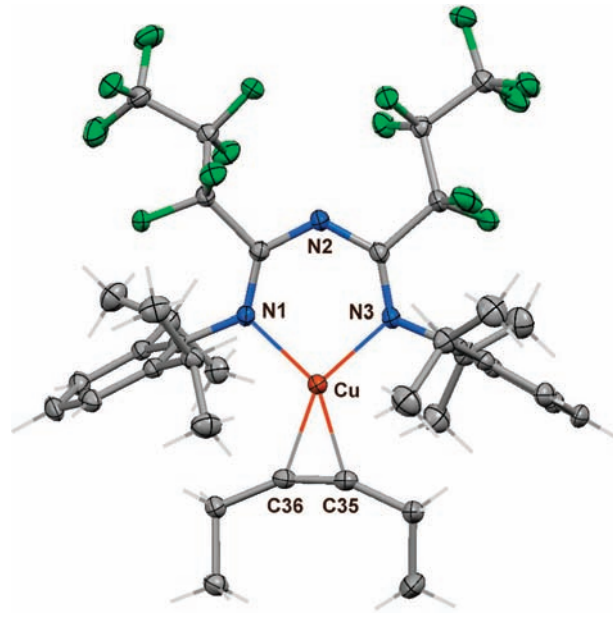

Figure 4. Molecular structure of [N{(C$_3$F$_7$)C(Dipp)N}$_2$]Cu(EtC≡CEt) (**7**). Thermal ellipsoids drawn at the 50% level. Selected bond lengths (Å) and angles (deg): Cu−N(3) 1.9624(15), Cu−N(1) 1.9635(15), Cu−C(35) 1.983(2), Cu−C(36) 1.9856(19), C(35)−C(36) 1.233(3); N(3)−Cu−N(1) 94.02(6), C(35)−Cu−C(36) 36.20(8), C(36)−C(35)−C(34) 156.5(2), C(35)−C(36)−C(37) 156.3(2).

Table 1. Summary of Experimental X-ray Crystallographic and Raman Data for [N{(C$_3$F$_7$)C(Dipp)N}$_2$]M(EtC≡CEt)[a]

parameter	**5** (M = **Au**)	**6** (M = **Ag**)	**7** (M = **Cu**)
d C≡C (Å)	1.233 (7)	1.216 (3)	1.233 (3)
d C≡C (Å)	*1.269*	*1.237*	*1.246*
d M−C (Å)	2.069 (4)	2.233 (2)	1.983 (2)
	2.071 (4)	2.241 (2)	1.9856 (19)
d M−C (Å)	*2.121*	*2.349*	*2.069*
d M−N (Å)	2.153 (3)	2.2026 (18)	1.9624 (15)
	2.155 (3)	2.2027 (17)	1.9635 (15)
d M−N (Å)	*2.235*	*2.262*	*2.016*
∠ C−C≡C (deg)	155.0 (4)	164.7 (2)	156.5 (2)
	155.7 (5)	165.3 (2)	156.3 (2)
∠ C−C≡C (deg)	*154.7*	*167.5*	*160.6*
∠ C−M−C (deg)	34.66 (18)	31.54 (8)	36.20 (8)
∠ N−M−N (deg)	85.31 (13)	85.03 (6)	94.02 (6)
$\bar{\nu}_{C\equiv C}$ (cm^{-1})	1920	2104	2003
$\bar{\nu}_{C\equiv C}$ *(cm^{-1})*	*1985*	*2151*	*2096*

[a] Results of DFT calculations (B3LYP/ccPVDZ) of model complexes [N{(CF$_3$)C(C$_6$H$_5$)N}$_2$]M(EtC≡CEt) are given in italicized letters and numerals. The calculated C≡C bond distance and $\bar{\nu}_{C\equiv C}$ of the free 3-hexyne are 1.215 Å and 2287 cm^{-1}, respectively.

C≡C bonds. However, the differences between the three adducts are not large enough to consider as significant at the 3σ level of estimated standard deviation. The C≡C−C angles in **5**−**7**, in contrast, show significant deviations from linearity, with the Au adduct showing the largest distortion, closely followed by the Cu and then Ag. Although, the steric effects can influence this parameter, such effects are expected to be highest for the copper system (not for Au), given the short Cu−C and Cu−N distances. The $\nu_{C\equiv C}$ bands of **5**−**7** can be observed in Raman (which is strong for the gold adduct but rather weak in the analogous Ag and Cu adducts; this is also true for the $\nu_{C\equiv C}$ bands in the IR) at 1920, 2104, and 2003 cm^{-1}, respectively. The Raman spectrum of the free 3-hexyne is somewhat complicated in the $\nu_{C\equiv C}$ region due to Fermi

(29) Cordero, B.; Gomez, V.; Platero-Prats, A. E.; Reves, M.; Echeverria, J.; Cremades, E.; Barragan, F.; Alvarez, S. *Dalton Trans.* **2008**, 2832–2838.
(30) Gordon, A. J.; Ford, R. A. *The Chemist's Companion*; Wiley: New York, 1972; p 108.

coupling,[9,32,33] and displays three bands at 2228, 2244, and 2296 cm^{-1}. We could not observe the $\nu_{C\equiv C}$ band of the 3-hexyne in the IR, but it has been reported at 2120 cm^{-1}.[34] Thus, relative to the free ligand peak positions, the gold adduct shows the largest lowering of the stretching frequency. This observation coupled with the C≡C−C bond angle data points to the presence of the most weakened C≡C bond in **5** as a result of metal ion coordination. Overall, Raman and X-ray data suggest that the combined effect of the alkyne → M σ-bond and M → alkyne π-bond is greatest for Au, followed by Cu and Ag.

We also investigated structures, bonding, and group trends of these metal alkyne adducts using density functional theory (DFT). To facilitate the calculations, we chose model compounds [N{$(CF_3)C(C_6H_5)N$}$_2$]M(EtC≡CEt) (M = Au, Ag, Cu). All molecules were fully optimized at the B3LYP/LANL2DZ (metal), ccpVDZ(C,N,F,H), level of theory. After relaxation the model compounds adopt C_s-symmetry, established by vibrational analysis. The computed structural data (summarized in Table 1) nicely follow the experimental trends. Results show that gold(I) affects the geometry of the 3-hexyne molecule the most, silver(I) the least, and copper(I) in between. This is apparent in the C≡C bond length, the C−C≡C angle, and the C≡C stretching vibration.

Enthalpies of formation of the model complexes [N{$(CF_3)C(C_6H_5)N$}$_2$]M(EtC≡CEt), computed between 3-hexyne on one side and the [N{$(CF_3)C(C_6H_5)N$}$_2$]M fragment on the other, are −153, −87, and −108 kJ/mol for Au, Ag, and Cu, respectively. The trend in formation enthalpy is paralleled by the magnitudes of the alkyne → metal σ-donation, 459, 132, and 221 kJ/mol, as well as the metal → alkyne π-back-donation, 201, 51, and 81 kJ/mol, for Au, Ag, and Cu, respectively. Furthermore, in all three adducts, the σ-component dominates over the π-back bonding component. The energy partition analysis of cationic, monocoordinate species $[M(HC\equiv CH)]^+$ also shows a similar pattern.[35] These calculated values, which increase in the order Ag < Cu < Au, indicate that gold(I) forms the strongest alkyne adducts while silver(I) forms the weakest. Furthermore, they also explain the observed trends in experimental and computed structural and vibrational data of the coordinated alkyne moiety, because stronger alkyne → metal σ-donation and metal → alkyne π-back-donation lead to a longer C≡C bond length, greater deviation from the linear C−C≡C angle (i.e., smaller angle), and a larger reduction in the C≡C stretching frequency.

A comparison between the trigonal-planar [N{$(CF_3)C(C_6H_5)N$}$_2$]M(EtC≡CEt) and the linear M(EtC≡CEt)Cl (where the triazapentadienyl ligand is replaced by a simple Cl as in the recently synthesized Au(EtC≡CEt)Cl)[18] yields the following additional observation. With Ag and Cu, bonding (σ-donation and π-back-donation) between metal and alkyne does not depend significantly on the anionic auxiliary triazapentadienyl or chloride ligand. The gold, however, shows a strong dependency of its bonding interaction to the alkyne with the choice of secondary donor. Relatively stronger σ- and π-components between the gold and alkyne were observed for the triazapentadienyl system. This is reflected in a shorter Au−C distance of 2.121 Å and a smaller C−C≡C angle of 154.7° for [N{$(CF_3)C(C_6H_5)N$}$_2$]Au(EtC≡CEt) in comparison to the corresponding values of 2.215 Å and 164.2° for Au(EtC≡CEt)Cl, despite the former having the larger coordination number. The increase in interaction between the alkyne π-system and the metal causes a longer C≡C bond (and lower bond order) and, as a consequence, a lower C≡C stretching frequency (calculated $\bar{\nu}_{C\equiv C}$ value of 1985 cm^{-1} for [N{$(CF_3)C(C_6H_5)N$}$_2$]Au(EtC≡CEt) in comparison to 2101 cm^{-1} of Au(EtC≡CEt)Cl). This trend is seen experimentally, as well, for the gold adducts (the analogous CuCl and AgCl adducts are unknown for a comparison). For example, the average Au−C distance and C−C≡C angle of [N{$(C_3F_7)C(Dipp)N$}$_2$]Au(EtC≡CEt) and Au(EtC≡CEt)Cl are 2.070 Å, 155.4° and 2.162 Å, 164.9°, respectively. Overall, the triazapentadienyl supporting ligand appears to prepare the frontier orbitals at the gold(I) for optimum interaction with the alkyne. This corroborates that covalent contributions play an important role in gold alkyne adduct formation.[35]

We have also estimated the energy required to rotate the alkyne moiety in the model system [N{$(CF_3)C(C_6H_5)N$}$_2$]M(EtC≡CEt). DFT calculations show that the experimentally observed structures with essentially coplanar N_2M and MC_2 triangles are significantly stable compared to conformers with 90° N_2M and MC_2 dihedral angles (i.e., tetrahedral N_2MC_2 arrangement) for all three coinage metal adducts. The gold adduct has the highest energy difference between the two conformers (61 kJ/mol) followed by the copper and silver, 26 and 19 kJ/mol, respectively. This trend is consistent with the computed M−alkyne bond energies.

It is also known that triazapentadienyl ligands can coordinate to metal ions in several different fashions.[24,25,36−40] For example, in addition to the κ^2-bonded triazapentadienyl ligand systems described in this contribution or as in [N{$(C_3F_7)C(2,6\text{-}Cl_2C_6H_3)N$}$_2$]Au($C_2H_4$),[26] κ^1-bonding via a terminal nitrogen atom (as in [$(C_6H_5)N(C_3F_7)CN(C_3F_7)C(C_6H_5)N$]HgMe based on solution NMR data)[38] or the central nitrogen atom (as in MeHg[N{$(C_3F_7)C(C_6H_5)N$}$_2$] and Tl[N{$(C_3F_7)C(Dipp)N$}$_2$] and ^{t}BuNCAg[N{$(C_3F_7)C(Dipp)N$}$_2$])[24,36,38] are known. Considering that gold(I) has a significantly greater tendency to appear as two- rather than three- or four-coordinate complexes,[27] we investigated energies of isomeric forms that could result from the interaction of (EtC≡CEt)Au^+ and [N{$(CF_3)C(C_6H_5)N$}$_2$]$^-$ fragments. Interestingly, the experimentally observed bonding mode (κ^2-bonded ligand involving two terminal nitrogen atoms leading to six-membered AuN_3C_2 metallacycle) has the lowest energy (see Supporting Information). In fact, two-coordinate, κ^1-bonded isomers involving the coordination of [N{$(CF_3)C(C_6H_5)N$}$_2$]$^-$ to the (EtC≡CEt)Au^+ fragment via the central nitrogen or one of the terminal nitrogens have energies even higher than that found for a κ^2-bonded system with a four-membered AuN_2C metallacycle involving one of the terminal nitrogen atoms and the central nitrogen atom.

(31) Boese, R.; Blaser, D.; Latz, R.; Baumen, A. *Acta Crystallogr.* **1999**, *C55*, IUC9900016.
(32) Crowder, G. A.; Blankenship, P. *J. Mol. Struct.* **1987**, *156*, 147–150.
(33) Lavalley, J. C.; Saussey, J.; Lamotte, J. *Spectrochim. Acta, Part A* **1979**, *35A*, 695–700.
(34) Yu, Y.; Smith, J. M.; Flaschenriem, C. J.; Holland, P. L. *Inorg. Chem.* **2006**, *45*, 5742–5751.
(35) Nechaev, M. S.; Rayon, V. M.; Frenking, G. *J. Phys. Chem. A* **2004**, *108*, 3134–3142.
(36) Dias, H. V. R.; Singh, S.; Cundari, T. R. *Angew. Chem., Int. Ed.* **2005**, *44*, 4907–4910.
(37) Dias, H. V. R.; Singh, S.; Flores, J. A. *Inorg. Chem.* **2006**, *45*, 8859–8861.
(38) Siedle, A. R.; Webb, R. J.; Brostrom, M.; Newmark, R. A.; Behr, F. E.; Young, V. G., Jr. *Organometallics* **2004**, *23*, 2281–2286.
(39) Siedle, A. R.; Webb, R. J.; Behr, F. E.; Newmark, R. A.; Weil, D. A.; Erickson, K.; Naujok, R.; Brostrom, M.; Mueller, M.; Chou, S.-H.; Young, V. G., Jr. *Inorg. Chem.* **2003**, *42*, 932–934.
(40) Dias, H. V. R.; Singh, S. *Dalton Trans.* **2006**, 1995–2000.

Unlike the *coinage metal alkynes* **5**−**7**, a complete series of *coinage metal alkenes* involving triazapentadienyl ligand auxiliaries are not available to examine coinage metal family group trends, but the gold− and copper−ethylene adducts [N{(C_3F_7)C(2,6-$Cl_2C_6H_3$)N}$_2$]Au(C_2H_4) and [N{(C_3F_7)C(2,6-$Cl_2C_6H_3$)N}$_2$]Cu(C_2H_4) are known.[26] They are monomeric and feature κ^2-bonded triazapentadienyl ligands and trigonal-planar metal sites. The ^{13}C NMR signal of the coordinated ethylene in the gold adduct appears at a significantly upfield position (59.1 ppm) relative to the free ethylene signal (123.3 ppm). The ethylene carbon resonance of the copper adduct [N{(C_3F_7)C(2,6-$Cl_2C_6H_3$)N}$_2$]Cu(C_2H_4) appears at 84.2 ppm, which is a relatively smaller upfield shift. A well-authenticated isoleptic series of coinage metal monoalkenes has been reported in the tris(pyrazolyl)borate ligand family.[14,41−44] However, they have different coordination geometries. For example, [HB(3,5-(CF_3)$_2$Pz)$_3$]Cu(C_2H_4) and [HB(3,5-(CF_3)$_2$Pz)$_3$]Ag(C_2H_4) have four-coordinate, pseudo-tetrahedral metal sites,[14,44] while the gold adduct [HB(3,5-(CF_3)$_2$Pz)$_3$]Au(C_2H_4)[43] features a three-coordinate, trigonal-planar metal site. Nevertheless, M−N and M−C bond lengths of these adducts follow the same trend as the covalent radii of M(I) (e.g., Cu−C < Au−C < Ag−C), which is similar to the trend observed for [N{(C_3F_7)C(Dipp)N}$_2$]M(EtC≡CEt) series. The upfield shift of the coordinated ethylene ^{13}C signal in [HB(3,5-(CF_3)$_2$Pz)$_3$]M(C_2H_4) relative to that of free ethylene is highest in the gold adduct (60 ppm shift) followed by the copper (34 ppm shift) and silver (19 ppm shift). The ^{13}C acetylenic resonance of the coordinated alkyne in [N{(C_3F_7)C(Dipp)N}$_2$]M(EtC≡CEt), in contrast, displays downfield shifts relative to that of free 3-hexyne in the copper and gold complexes or shows essentially no change in the silver adduct.

In summary, we describe the isolation of the first truly isoleptic series of coinage metal alkynes. The use of the fluorinated 1,3,5-triazapentadienyl auxiliary ligand [N{(C_3F_7)C(Dipp)N}$_2$]$^-$, afforded thermally stable 3-hexyne complexes of gold(I), silver(I), and copper(I). These adducts have similar crystals structures. [N{(C_3F_7)C(Dipp)N}$_2$]Au(EtC≡CEt) represents a relatively less common trigonal-planar gold complex. The M−C and M−N bond distances of [N{(C_3F_7)C(Dipp)N}$_2$]M(EtC≡CEt) vary in the order Cu < Au < Ag. The C−C≡C bond angle shows the largest deviation from linearity in the gold, then in the Cu and Ag adducts. The gold complex also shows the largest decrease in C≡C stretching frequency, followed by Cu and Ag adducts. DFT calculations show that the gold(I) forms the strongest bond with the alkyne, while the silver(I) forms the weakest bond. Furthermore, in these triazapentadienyl coinage metal adducts, the σ-donation from alkyne → M dominates over the M → alkyne π-back-donation. Coinage metal ions, and in particular gold, are widely used as effective π-activation catalysts for alkynes, and [N{(C_3F_7)C(Dipp)N}$_2$]M(EtC≡CEt) complexes may be viewed as good models for likely intermediates in some of these processes. We are currently exploring the reactivity of complexes **5**−**7** and investigating the chemistry between coinage metal ions and various other alkynes (and alkenes).

Experimental Section

General Procedures. All manipulations were carried out under an atmosphere of purified nitrogen using standard Schlenk techniques or in a Drybox. Reactions involving gold(I) and silver(I) starting materials were performed in flasks covered with aluminum foil (to protect from light). Solvents were purchased from commercial sources, purified using Innovative Technology SPS-400 PureSolv solvent drying system or by distilling over conventional drying agents and degassed by the freeze−pump−thaw method prior to use. Glassware was oven-dried at 150 °C overnight. NMR spectra were recorded in C_6D_{12} and $CDCl_3$ at 25 °C on a JEOL Eclipse 500 spectrometer (^{1}H: 500.16 MHz; ^{13}C: 125.77 MHz; ^{19}F: 470.62 MHz). Proton and carbon chemical shifts are reported in ppm versus Me_4Si, and referenced using the residual proton or carbon signals (C_6D_{12}: ^{1}H, δ 1.38; ^{13}C, δ 26.43 and $CDCl_3$: ^{1}H, δ 7.24; ^{13}C, δ 77.23) of the deuterated solvent. ^{19}F NMR chemical shifts were referenced relative to external $CFCl_3$. Elemental analyses were performed using a Perkin-Elmer series II CHNS/O analyzer. Melting points were obtained on a Mel-Temp II apparatus and were not corrected. Infrared spectra were recorded at 25 °C on a JASCO FT-IR 410 spectrometer. Raman spectra were recorded at 25 °C on Horiba Jobin Yvon LabRAM Aramis Raman spectrometer instrument using a 633 nm laser source and pure crystalline material of the metal complexes. *n*-Butyllithium (1.6 M in hexanes), $(CuOTf)_2$·benzene, gold(I) chloride, silver(I) triflate, and 3-hexyne were purchased from commercial sources. [N{(C_3F_7)C(Dipp)N}$_2$]H (Dipp = 2,6-diisopropylphenyl) was synthesized using a published procedure.[24] For comparison, free 3-hexyne: ^{1}H NMR (C_6D_{12}, 298 K): δ 2.07 (CH_2, 4H, apparent quartet of triplet, J = 7.5 Hz, J = 2.1 Hz), 1.06 (CH_3, 6H, t, J = 7.5 Hz), and ^{13}C{^{1}H} NMR (C_6D_{12}, 298 K): δ 80.7 (C≡C), 14.8, 13.1; ^{1}H NMR ($CDCl_3$, 298 K): δ 2.13 (CH_2, 4H, apparent quartet of triplet, J = 7.5 Hz, J = 2.1 Hz), 1.09 (CH_3, 6H, t, J = 7.5 Hz), and ^{13}C{^{1}H} NMR ($CDCl_3$, 298 K): δ 81.0 (C≡C), 14.5, 12.5; Raman (cm^{-1}): 2976, 2938, 2919, 2907, 2880, 2851, 2296, 2244, 2228, 1440, 1317, 1063, 979, 916, 781, 683 (see Supporting Information for additional details).

[N{(C_3F_7)C(Dipp)N}$_2$]Li. [N{(C_3F_7)C(Dipp)N}$_2$]H (0.232 g, 0.32 mmol) was dissolved in diethyl ether (30 mL) and cooled to −60 °C. To this solution, ^{n}BuLi (0.20 mL, 1.6 M in hexanes) was added dropwise, and then the mixture was allowed to warm to the room temperature and stirred for a further 2 h. The volatile materials were removed under reduced pressure, and the resulting residue was dried under vacuum for 2 h. *n*-Hexane (10 mL) was added to the residue, the mixture stirred for 20 min, and volatile materials were removed under vacuum (∼1 h) to obtain solid [N{(C_3F_7)C(Dipp)N}$_2$]Li as much as possible or completely free of diethyl ether. This lithium salt was used directly in the following procedures.

[N{(C_3F_7)C(Dipp)N}$_2$]Au(EtC≡CEt) (5). [N{(C_3F_7)C(Dipp)N}$_2$]Li (0.32 mmol) was dissolved in *n*-hexane (15 mL), and 3-hexyne (0.04 mL, 0.32 mmol) was added using a syringe. This solution was cooled at −10 °C and transferred to a flask containing AuCl (0.074 g, 0.32 mmol). This mixture was stirred for 20 min at ∼7 °C (important to maintain the temperature below 10 °C to avoid decomposition). Once the solution started to turn purple, the stirring was stopped, and the solution was filtered over a bed of Celite. The filtrate was collected and concentrated to ∼1 mL at 0 °C by slow evaporation under reduced pressure. It was then placed in a −20 °C freezer to obtain yellow-greenish crystals of [N{(C_3F_7)C(Dipp)N}$_2$]Au(EtC≡CEt) within a day. The solution was removed using a syringe, and the crystals were dried under reduced pressure. Yield: 85%, Mp: darkens at 110 °C, melted 157−164 °C (dec).^{1}H NMR (C_6D_{12}): δ 7.01 (m, 6H, *m*,*p*-Ar), 3.18 (septet, 4H, J = 6.9 Hz, C*H*(CH_3)$_2$), 1.25 (d, 12H, J = 6.9 Hz, CH(C*H*$_3$)$_2$), 1.17 (d, 12H, J = 6.9 Hz, CH(C*H*$_3$)$_2$), 1.10 (quartet, 4H, J = 7.4 Hz, $C_2CH_2CH_3$), 0.79 (triplet, 6H, J = 7.4 Hz, $C_2CH_2CH_3$). ^{13}C{^{1}H}

(41) Dias, H. V. R.; Wu, J. *Eur. J. Inorg. Chem.* **2008**, 509–522. Dias, H. V. R.; Wu, J. *Eur. J. Inorg. Chem.* **2008**, 2113.
(42) Dias, H. V. R.; Lovely, C. J. *Chem. Rev.* **2008**, *108*, 3223–3238.
(43) Dias, H. V. R.; Wu, J. *Angew. Chem., Int. Ed.* **2007**, *46*, 7814–7816.
(44) Dias, H. V. R.; Lu, H.-L.; Kim, H.-J.; Polach, S. A.; Goh, T. K. H. H.; Browning, R. G.; Lovely, C. J. *Organometallics* **2002**, *21*, 1466–1473.

NMR (C_6D_{12}) coordinated 3-hexyne signals: 91.3 (s, Et*C*≡*C*Et), 14.4, 12.3. ^{19}F NMR (C_6D_{12}): δ −81.26 (triplet, 6F, J_{FF} = 10.8 Hz, CF_3), −106.02 (quartet, 4F, J_{FF} = 10.8 Hz, α-CF_2), −122.55 (s, 4F, β-CF_2). ^{1}H NMR ($CDCl_3$): δ 7.04 (s, 6H, *m*,*p*-Ar), 3.11 (septet, 4H, J = 6.9 Hz, C*H*(CH_3)$_2$), 1.23 (d, 12H, J = 6.9 Hz, CH(C*H*$_3$)$_2$), 1.13 (d, 12H, J = 6.9 Hz, CH(C*H*$_3$)$_2$), 1.04 (quartet, 4H, J = 7.4 Hz, $C_2CH_2CH_3$), 0.79 (triplet, 6H, J = 7.4 Hz, $C_2CH_2CH_3$). ^{13}C{^{1}H} NMR ($CDCl_3$) selected: 90.3 (s, Et*C*≡*C*Et). ^{19}F NMR ($CDCl_3$): δ −80.34 (triplet, 6F, J_{FF} = 10.1 Hz, CF_3), −105.64 (quartet, 4F, J_{FF} = 10.1 Hz, α-CF_2), −122.19 (s, 4F, β-CF_2). Anal. Calcd for $C_{38}H_{44}N_3F_{14}Au$: C, 45.38; H, 4.41; N, 4.18. Found: C, 45.90; H, 4.71; N, 4.16. IR (Nujol, cm^{-1}) selected: 1923 (m, C≡C); IR (KBr, cm^{-1}): 1924 (m, C≡C). Raman (cm^{-1}): 1920 (m, C≡C). Crystals of [N{(C_3F_7)C(Dipp)N}$_2$]Au(EtC≡CEt) are air and light stable for well over 24 h. A solution of the title compound in $CDCl_3$ is also stable for more than 24 h under darkness at room temperature.

[N{(C_3F_7)C(Dipp)N}$_2$]Ag(EtC≡CEt) (6). [N{(C_3F_7)C(Dipp)-N}$_2$]Li (0.32 mmol) was dissolved in *n*-hexane (15 mL), and 3-hexyne (0.04 mL, 0.32 mmol) was added using a syringe. This solution was cooled to −10 °C and transferred to a flask containing AgOTf (0.082 g, 0.32 mmol). The mixture was stirred for 20 min at <5 °C (it is important to maintain the low temperature; longer stirring times should also be avoided as it leads to darker solutions, perhaps indicating some decomposition). It was filtered over a bed of Celite, and the filtrate was collected and concentrated to ∼1 mL at 0 °C by passing a nitrogen stream. The resulting solution was cooled at −20 °C to obtain [N{(C_3F_7)C(Dipp)N}$_2$]Ag(EtC≡CEt) as pale-yellow crystals in about 6 h. The solution was removed using a syringe, and the crystals were separated and dried under reduced pressure. Yield: 72%, Mp: changes color at 109 °C, darkens at 121 °C, melted 163−166 °C (dec).^{1}H NMR (C_6D_{12}): δ 6.98 (d, 4H, 7.8 Hz, *m* -Ar), 6.90 (t, 2H, 7.8 Hz, *p*-Ar), 3.21 (septet, 4H, J = 6.9 Hz, C*H*(CH_3)$_2$), 1.25 (d, 12H, J = 6.9 Hz, CH(C*H*$_3$)$_2$), 1.17 (d, 12H, J = 6.9 Hz, CH(C*H*$_3$)$_2$), 0.98 (quartet, 4H, J = 6.9 Hz, $C_2CH_2CH_3$), 0.74 (triplet, 6H, J = 6.9 Hz, $C_2CH_2CH_3$). ^{13}C{^{1}H} NMR (C_6D_{12}) coordinated 3-hexyne signals: 80.6 (s, Et*C*≡*C*Et), 14.8, 13.2. ^{19}F NMR (C_6D_{12}): δ −81.32 (triplet, 6F, J_{FF} = 9.0 Hz, CF_3), −106.36 (quartet, 4F, J_{FF} = 9.0 Hz, α-CF_2), −122.68 (s, 4F, β-CF_2). ^{1}H NMR ($CDCl_3$): δ 7.03 to 6.95 (m, 6H, *m*,*p*-Ar), 3.14 (septet, 4H, J = 6.9 Hz, C*H*(CH_3)$_2$), 1.24 (d, 12H, J = 6.9 Hz, CH(C*H*$_3$)$_2$), 1.14 (d, 12H, J = 6.9 Hz, CH(C*H*$_3$)$_2$), 0.92 (br, 4H, $C_2CH_2CH_3$), 0.75 (apparent triplet, 6H, $C_2CH_2CH_3$). ^{13}C{^{1}H} NMR ($CDCl_3$) selected: 80.9 (s, Et*C*≡*C*Et). ^{19}F NMR ($CDCl_3$): δ −80.41 (triplet, 6F, J_{FF} = 10.1 Hz, CF_3), −105.96 (quartet, 4F, J_{FF} = 10.1 Hz, α-CF_2), −122.31 (s, 4F, β-CF_2). Anal. Calcd for $C_{38}H_{44}N_3F_{14}Ag$: C, 49.79; H, 4.84; N, 4.58. Found: C, 50.01; H, 4.77; N, 4.58. IR (Nujol, cm^{-1}) selected: 2105 (weak); IR (KBr, cm^{-1}) selected: 2122−2104 (weak br). Raman (cm^{-1}): 2104 (w, C≡C). Crystals of [N{(C_3F_7)C(Dipp)N}$_2$]Ag(EtC≡CEt) are air and light stable for more than 24 h. Darkening is observed after about 3 days. No decomposition was observed for more than 2 weeks at −20 °C under inert atmosphere in the presence of *n*-hexane. However, the product decomposes slowly in $CDCl_3$ even in the dark at room temperature, as evident from the formation of a black solid.

[N{(C_3F_7)C(Dipp)N}$_2$]Cu(EtC≡CEt) (7). [N{(C_3F_7)C(Dipp)N}$_2$] Li (0.32 mmol) was dissolved in *n*-hexane (15 mL), and 3-hexyne (0.04 mL, 0.32 mmol) was added via a syringe. This solution was cooled at 0 °C and then transferred to a flask containing $(CuOTf)_2$·benzene (0.081 g, 0.16 mmol). The mixture was stirred for 90 min at 5 °C (the solution turned cloudy). The stirring was stopped, and the solution was filtered over a bed of Celite. The filtrate was collected and concentrated to ∼1 mL at 5 °C by slow evaporation under reduced pressure. It was cooled at −20 °C to obtain yellow-greenish crystals of [N{(C_3F_7)C(Dipp)N}$_2$]Cu(EtC≡CEt) overnight. The supernatant was removed using a syringe, and the crystals were dried under reduced pressure. Yield: 80%, Mp: darkens at 133 °C, melted 140−147 °C (dec).^{1}H NMR (C_6D_{12}): δ 7.01 (m, 6H, *m*,*p*-Ar), 3.09 (septet, 4H, J = 6.9 Hz, C*H*(CH_3)$_2$), 1.24 (d, 12H, J = 6.9 Hz, CH(C*H*$_3$)$_2$), 1.14 (d, 12H, J = 6.9 Hz, CH(C*H*$_3$)$_2$), 0.80 (br quartet, 4H, $C_2CH_2CH_3$), 0.76 (br triplet, 6H, $C_2CH_2CH_3$). ^{13}C{^{1}H} NMR (C_6D_{12}) coordinated 3-hexyne signals: 99.2 (s, Et*C*≡*C*Et), 15.4, 13.5. ^{19}F NMR (C_6D_{12}): δ −81.22 (triplet, 6F, J_{FF} = 10.8 Hz, CF_3), −105.58 (quartet, 4F, J_{FF} = 10.8 Hz, α-CF_2), −122.31 (s, 4F, β-CF_2). ^{1}H NMR ($CDCl_3$): δ 7.05 (s, 6H, *m*,*p*-Ar), 3.02 (septet, 4H, J = 6.9 Hz, C*H*(CH_3)$_2$), 1.23 (d, 12H, J = 6.9 Hz, CH(C*H*$_3$)$_2$), 1.10 (d, 12H, J = 6.9 Hz, CH(C*H*$_3$)$_2$), 0.75 (br singlet, 4H, CH_2CH_3), 0.75 (br singlet, 6H, CH_2CH_3). ^{13}C{^{1}H} NMR ($CDCl_3$) selected: 98.2 (s, Et*C*≡*C*Et). ^{19}F NMR ($CDCl_3$): δ −80.31 (triplet, 6F, J_{FF} = 10.7 Hz, CF_3), −105.20 (quartet, 4F, J_{FF} = 10.7 Hz, α-CF_2), −121.96 (s, 4F, β-CF_2). Anal. Calcd for $C_{38}H_{44}N_3F_{14}Cu$: C, 52.32; H, 5.08; N, 4.82. Found: C, 52.57; H, 5.12; N, 4.82. IR (Nujol, cm^{-1}) selected: 2045 (vw), 2008 (w); IR (KBr, cm^{-1}) selected: 2044 (vw), 2007 (w). Raman bands in the 1750−2500 region (cm^{-1}): 2003 (w, C≡C), 2039 vw. Crystals are air and light stable for more than 24 h. These show no decomposition at −20 °C under inert atmosphere in the presence of *n*-hexane after 1 week. A solution of the title compound in $CDCl_3$ darkens after 12 h at room temperature.

X-ray Crystallographic Data. X-ray quality crystals of **5**−**7** were obtained from hexane solutions at −20 °C. A suitable crystal covered with a layer of hydrocarbon/paratone-N oil was selected and mounted on a Cryo-loop, and immediately placed in the low-temperature nitrogen stream. The X-ray intensity data were measured at 100(2) K on a Bruker SMART APEX CCD area detector system equipped with a Oxford Cryosystems 700 series cooler, a graphite monochromator, and a Mo Kα fine-focus sealed tube (λ = 0.710 73 Å). The data frames were integrated with the Bruker SAINT-Plus (version 6.45) software package. Structures were solved and refined using Bruker SHELXTL (version 6.14) software package. All the non-hydrogen atoms were refined anisotropically. Hydrogen atoms were placed at calculated positions and refined riding on the corresponding carbons. The CCDC 731649, 73150, and 731651 contain the supplementary crystallographic data for compounds **7** (copper adduct), **6** (silver adduct), and **5** (gold adduct), respectively. Some of these data are given in Tables S1−6, Supporting Information.

Crystal Data of [N{(C_3F_7)C(Dipp)N}$_2$]Au(EtC≡CEt) (5). Empirical formula $C_{38}H_{44}AuF_{14}N_3$, FW = 1005.73, Temp = 100(2) K, Crystal system = Triclinic, Space gp = $P\bar{1}$, a = 9.0868(3) Å, b = 12.6753(5) Å, c = 17.8359(7) Å, α = 82.848(1)°, β = 78.796(1)°, γ = 80.426(1)°, Volume = 1978.04(13) Å^3, Z = 2, Final R indices [$I > 2\sigma(I)$] R1 = 0.0320, wR2 = 0.0864; R indices (all data) R1 = 0.0323, wR2 = 0.0866.

Crystal Data of [N{(C_3F_7)C(Dipp)N}$_2$]Ag(EtC≡CEt) (6). Empirical formula $C_{38}H_{44}AgF_{14}N_3$, FW = 916.63, Temp = 100(2) K, Crystal system = Triclinic, Space gp = $P\bar{1}$, a = 9.1356(6) Å, b = 12.7961(9) Å, c = 17.7376(12) Å, α = 82.756(1)°, β = 78.647(1)°, γ = 80.038(1)°, Volume = 1993.2(2) Å^3, Z = 2, Final R indices [I > 2σ(I)] R1 = 0.0333, wR2 = 0.0852; R indices (all data) R1 = 0.0355, wR2 = 0.0869.

Crystal Data of [N{(C_3F_7)C(Dipp)N}$_2$]Cu(EtC≡CEt) (7). Empirical formula $C_{38}H_{44}CuF_{14}N_3$, FW = 872.30, Temp = 100(2) K, Crystal system = Triclinic, Space gp = $P\bar{1}$, a = 9.1036(3) Å, b = 12.5604(5) Å, c = 17.6485(6) Å, α = 81.606(1)°, β = 79.605(1)°, γ = 80.286(1)°, Volume = 1942.49(12) Å^3, Z = 2, Final R indices [$I > 2\sigma(I)$] R1 = 0.0379, wR2 = 0.0997; R indices (all data) R1 = 0.0414, wR2 = 0.1025.

Computational Study. Density functional calculations were performed using the B3LYP functional as implemented in Gaussian 03.[45] We choose cc-pVDZ basis sets for main group elements and LANL2DZ basis sets for metal atoms. For Cl we added polarization functions. For the model compounds [N{(CF_3)C(C_6H_5)N}$_2$] M(EtC≡CEt) (M = Au, Ag, Cu) we found minimum structures in C_s-symmetry as indicated by the frequency analysis. A C_{2v}-

(45) Frisch, M. J.; et al. *Gaussian 03*, Revision D.02; Gaussian, Inc.: Wallingford CT, 2004.

symmetric model is very close in energy, but exhibits an imaginary frequency. It results in a kink of the N_3C_2 unit relative to the (alkyne-) C_2M fragment. Approaches to find lower-energy structures through distortions or rotations and subsequent optimizations all ended in this C_s-symmetric model. Thus, the alkyne-to-metal bonding is symmetrical (no slippage as previously found for Au(EtC≡CEt)Cl). In addition, this implies the 3-hexyne adopts C_s-symmetry upon coordination, while DFT locates the ground state of the free 3-hexyne in C_2-symmetry. Optimized structures were further analyzed using the formalism of natural bond orbitals (NBO).[46] Herein, we present magnitudes only for the most significant natural bond. A simple analysis and comparison is complicated by a manifold of interactions, especially for the copper adduct. The vibrational frequencies of the C≡C stretching (free ligand: 2287 cm^{-1}) is calculated using a scaling factor of 0.9709.[47]

Crystallographic Data. The crystallographic data have been deposited in the Cambridge Structural Database, Cambridge Crystallographic Data Center, Cambridge CB2 1EZ, United Kingdom, CSD reference numbers CCDC-731651 (**5**), CCDC-73150 (**6**), and CCDC-731649 (**7**). These data can be obtained free of charge from the Cambridge Crystallographic Data Center via www.ccdc.cam.ac.uk/data_request/cif.

Acknowledgment. This work has been supported by the Welch Foundation (HVRD: Y-1289).

Supporting Information Available: Further structural details, figures and computational results including Cartesian coordinates and energies of optimized geometries; complete citations for ref 45; X-ray crystallographic data. This material is available free of charge via the Internet at http://pubs.acs.org.

JA904232V

(46) Reed, A. E.; Curtiss, L. A.; Weinhold, F. *Chem. Rev.* **1988**, *88*, 899–926.

(47) Sinha, P.; Boesch, S. E.; Gu, C.; Wheeler, R. A.; Wilson, A. K. *J. Phys. Chem. A* **2004**, *108*, 9213–9217.